8-2009

Analytical and Computational Studies of Magneto-Convection in Solidifying Mushy Layer

Mallikarjunaiah Siddapura Muddamallappa
University of Texas-Pan American

ANALYTICAL AND COMPUTATIONAL STUDIES OF MAGNETO-CONVECTION IN SOLIDIFYING MUSHY LAYER

A Thesis

by

MALLIKARJUNAIAH SIDDAPURA MUDDAMALLAPPA

Submitted to the Graduate School of the
University of Texas-Pan American
In partial fulfillment of the requirements for the degree of

MASTER OF SCIENCE

August 2009

Major Subject: Mathematics

ANALYTICAL AND COMPUTATIONAL STUDIES OF MAGNETO-CONVECTION IN SOLIDIFYING MUSHY LAYER

A Thesis
by
MALLIKARJUNAIAH SIDDAPURA MUDDAMALLAPPA

Approved as to style and content by:

Dr. Daniel N. Riahi
Chair of Committee

Dr. Dambaru Bhatta
Committee Member

Dr. Paul Bracken
Committee Member

Dr. Andras Balogh
Committee Member

August 2009

ABSTRACT

Muddamallappa, Mallikarjunaiah Siddapura, Analytical and computational studies of magneto-convection in solidifying mushy layer, Master of Science(MS), August 2009, 46 pages, 31 reference, 5 titles.

Natural convection in solidifying binary media is of great interest due to it's applications in material processing and crystal growth industries. Convective flows between the layers of melt during alloy solidification is known to produce mechanical imperfections such as freckle's. Hence it is important to investigate the criterion for freckling and discover the means of suppressing it.

A mushy layer, which has both solid and fluid components and is formed between underlying solid and overlying liquid, is known to produce chimneys, which are narrow, vertical vents, devoid of solid. We consider the problem of magneto-convection in a horizontal mushy layer during the solidification of binary alloys. Both cases of permeable and impermeable mush-liquid interface were investigated. We carry out the numerical investigation for particular range of parameter values which cover those of available experimental studies. Cases of constant and variable permeability coupled with mush-liquid interface boundary conditions were included in the present study. The governing coupled non-linear partial differential equations are non-dimensionalized and solved to get steady basic state solution. Using multiple shooting technique we determine the steady state solutions in a range of critical Rayleigh number. We analyse the effect of, Chandrasekhar number Q, far-field temperature, permeability of the medium, mush-liquid interface condition, on the problem. The results of the analysis and computation indicate that increasing Q has the stabilizing effect on the solidification, because the critical Rayleigh number increases with increasing the strength of magnetic field. But permeable mush-liquid interface condition destabilizes the convection by reducing the critical Rayleigh

number. It was also found that for moderate or small values of Robert's number, the critical Rayleigh number is mostly insensitive. The most important finding of the present investigation is that the convection in a mushy layer decreases upon increasing the strength of externally imposed magnetic field and increasing far-field temperature. These theoretical results have been observed in related experiments of damped magneto-convection by Vives and Perry (1987).

DEDICATION

This work is dedicated to my beloved parents Muddamallappa and Umadevi.

ACKNOWLEDGMENTS

First, I would like to thank my advisors, Dr. Daniel N. Riahi and Dr. Dambaru Bhatta, for enabling me to undertake these studies, for providing me with an interesting and challenging topic. Without their help and support this research would have been impossible. My thanks go to my thesis committee members: Dr. Paul Bracken, Dr. Andras Balogh for their suggestions. Also, I would like to express my thanks to Faculty Research Council of UTPA for the financial support for this project. My thanks also goes to my wife for her solid support over all these years.

DECLARATION

Some parts of the work presented in this thesis have been published/submitted in the following articles:

[1] Muddamallappa M. S., Bhatta D., Riahi D.N.(2009), Numerical investigation on marginal stability and convection with and without magnetic field in a mushy layer, *Transport in Porous Media*, 79: 301-317 .

[2] Muddamallappa M. S., Bhatta D., Riahi D.N., Linear convective stability in a mushy layer with non-uniform magnetic field and permeable mush-liquid interface, accepted for publication in *Journal of Porous Media.*

[3] Bhatta D., Muddamallappa M. S., Riahi D.N., on perturbation and marginal stability analysis of magneto-convection in active mushy layer, accepted for publication in *Transport in Porous Media.*

[4] Bhatta D., Muddamallappa M. S., Riahi D.N., Effect of non-uniform magnetic field on convective instability of a mushy layer with variable permeability, in review *International Journal of Engineering Science.*

TABLE OF CONTENTS

LIST OF FIGURES

Page

CHAPTER 1

INTRODUCTION

The area of solidification is becoming of great importance in real world applications with the advancement of technologies day by day. Solidification process is used in various fields such as manufacturing, material science, earth science, energy and environmental science. Crystal growth, ceramics, welding and castings are various applications in material science involving solidification. Volcanic systems, crystal magmas, ore deposits and sea ice are earth science related solidification applications. In engineering applications it is important to reduce the undesirable effects of convection in mushy layer and also find ways to prevent formation of localized chimneys within the mushy layer. Since it is known that chimney convection can lead to mechanical imperfections in the final form of solidified alloy, referred to as freckle's. In geological applications, a large amount of molten rock is produced within the earth and this melt solidifies in magma chambers, along lava flows and during the volcanic eruptions.

When a binary alloy is cooled from below, a distinct mushy layer made of dendritic crystals is formed due to morphological instabilities of the solid-liquid interface. Partially solidified, mush region is treated as a reactive porous medium. Convective flow in mushy layer causes freckles. Freckles are roughly cylindrical regions that are depleted in solute and often have anisotropically oriented grains. They form along the direction of solidification and cause a disruption of compositional homogeneity. Freckles are commonly found in cast binary alloys such as nickel-aluminum, aluminum-copper and lead-tin, as well as steel. Hence investigating the criteria and controlling natural convection in mushy layer is important in crystal growth processes for semi conductor industry.

The freckles were first reported by Copley et al (1970), during the unidirectional solidification of ammonium chloride and water solution. They concluded that freckle formation occurs more in the mushy zone with high thermal diffusivity, low solute diffusivity and low viscosity. Hills et al. (1983) developed a set of thermodynamic equations for a mushy layer and solved one dimensional freezing problem. Fowler (1985) developed a mathematical model for the convective

et al. (1983) developed a set of thermodynamic equations for a mushy layer and solved one dimensional freezing problem. Fowler (1985) developed a mathematical model for the convective flow in chimneys and predicted a criterion for the onset of convection and freckling. Huppert (1985) studied experimentally the six different cases that arise when homogeneous solution is cooled from below and also evaluated the criterion for which solid-liquid interface becomes unstable. Worster (1986) developed a model for dendritic growth that often formed during the solidification of binary alloy by considering the region of mixed phase as continuum and suggested different morphologies that can occur due to the variation of the solid fraction. Several experimental studies, concerning the solidification of binary alloy with or without magnetic field, are available in the literature. Vives and Perry (1987) carried out the experimental studies of natural and damped convection during the solidification of metal alloys. The damped convection was caused by a stationary and uniform magnetic field parallel to the gravity. They observed that the stationary magnetic field decreases the superheat and increases the rate of solidification. Vives (1990) examined the influence of rotating aluminium alloy flows, driven by a stationary electromagnetic field, during freezing in a toroidal mold. Chen and Chen (1991) conducted directional solidification experiments, without externally imposed magnetic field, using ammonium chloride-water solution, studied different types of convection and calculated the critical Rayleigh number of mushy layer for the onset of plume convection.

Many interesting and important, theoretical and experimental investigations concerning the convection within the mushy layer, which is responsible for the formation of chimneys, were reported during the last three decades. Worster (1991) developed and analyzed the governing equations for a mushy layer in the asymptotic limit of large solutal Rayleigh number. He observed that there is downward flow everywhere in the mushy region, except in and near the chimneys. He determined a critical Rayleigh number above which the mushy layer is unstable to small disturbances. Worster (1992) solved the linear stability problem for binary alloy solidification. He detected two modes of instabilities, one of which has been referred to as the mushy layer mode. This mode has a wavelength comparable to the depth of the mushy layer and is responsible for the development of chimneys within the mushy layer. The second mode of instability, which we referred to as the boundary-layer mode was found to have a wavelength comparable to the depth

of the compositional boundary layer above the mush-liquid interface. These results were obtained under the restriction of infinite Prandtl number. The mushy layer mode drives the convective flow downward everywhere except in and near the localized chimneys. This result is in agreement with the experimental result of Tait and Jaupart (1992a,b), in which they conducted experiments using aqueous solutions of ammonium chloride. In addition, these authors observed that the boundary layer at the top of the mush becomes unstable, leading to convection in the overlying fluid. They also observed that up flow occured at the cell boundaries and the down flow at the cell centers.

A notable simplified mushy-layer model was first introduced by Amberg and Homsy (1993). The model was based on a near eutectic approximation and in the limit of large far-field temperature. Such asymptotic limits allowed them to examine the dynamics of the mushy layer in the form of a small deviation from the classical system of convection in a horizontal porous medium with constant permeability. Emms and Fowler (1994) proposed a coupled mush-liquid model to study the onset of convection during the directional solidification of binary alloys. Anderson and Worster (1995) employed a weakly nonlinear analysis of simplified mushy layer model that was proposed by Amberg and Homsy (1993). They considered the limit of large Stefan number, which enabled them to reach a domain for the existence of the oscillatory mode of convection.

The experimental studies of directional solidification of binary alloys in the absence of magnetic field are due to Chen and Chen (1991) and Chen (1995). Chen and Chen (1991) conducted experiments by cooling sodium chloride and water solution from below at constant temperature. They used a Kozeny-Carman type of relation to calculate the permeability and found the critical solute Rayleigh number across the mushy layer for the onset of plume convection. Chen (1995) applied a dye tracing method to study convection within the mushy layer before and after the onset of plume convection and X-ray tomography to measure the solid fraction of a growing mush. It was reported that there was no convective motion in the mush prior to the onset of chimneys and the solid fraction of the mush decrease toward the bottom of the tank after the chimneys are fully developed.

Several attempts were made to study the solidification process by imposing certain external constraints, such as rotation and/or magnetic field, to suppress or at least reduce unwanted convection in the mushy layer. Riahi (1997) studied the effects of a high gravity environment, where

rotation serves as an external constraint, on natural convection in cylindrical chimneys within a mushy layer during the solidification of binary alloy. It was observed that for some moderate values of the rotation rate, axial convection in the chimneys decreases rapidly with increasing acceleration parameter and increasing Coriolis parameter. Riahi (2000) investigated, asymptotically, the effects of vertical magnetic field on the chimney convection in mushy layer. Three cases of magnetic field such as strong, moderate and weak were studied. The presence of an externally imposed magnetic field in the vertical direction was found to be stabilizing in the case of strong magnetic field and ineffective in the case of a moderate (or weak) magnetic field.

Riahi (2001) also studied non-linear buoyancy driven convection in the melt and in cylindrical chimneys in a mushy layer during alloy solidification, subjected to externally imposed strong magnetic field under the influence of centrifugal and Coriolis forces. It was found, in particular, that chimney convection generally decreases with increasing magnetic parameter Q (Chandrasekhar Number), and also chimney convection can have lower amplitude for certain ranges of the Coriolis force. Such theoretical results were found agreeable with some available experimental and computational results.

Okhuysen and Riahi (2008a), examined a weakly nonlinear analysis of buoyant convection in binary alloy solidification for permeable mush-liquid interface and in the absence of vertical magnetic field. They analyzed effects of several parameters on two and three-dimensional steady convection patterns in the mushy layers for variable permeability. The most important result of their study was the prediction of a subcritical down-hexagonal pattern for variable permeability case that corresponds to the smallest value of the Rayleigh number. Okhuysen and Riahi (2008b) analyzed the linear flow instabilities of the liquid and mushy regions during directional solidification of binary alloy under high gravity environment. Their linear stability analysis indicated the presence of mushy layer mode in the case of rotation. The chimney formation in mushy zone was found to be reduced by increasing the rotation rate.

To date, all the flow patterns observed by Tait and Jaupart (1992) remain unaccounted for in the theoretical study of such solidification problems. Among the theoretical and computational studies of nonlinear convection in mushy layers during solidification of alloys in the absence of externally imposed magnetic field that have been done so far, the one that actually predicted the

particular flow pattern observed in experiments (Tait and Jaupart, 1992) for flow regime near onset of motion, is that due to Okhuysen and Riahi (2008).

In Chapter 2 mathematical formulation of a single-layer mode of the mushy zone under the externally applied uniform magnetic field is provided. This model is the extension of previous asymptotic studies of Riahi (2000). First the geometry of the system under consideration is presented. Then, physical concepts are introduced and basic assumptions are discussed. The governing equations and boundary conditions for the problem are then formulated.

In Chapter 3, the system formulated in Chapter 2 is analyzed. For each case, linear stability is considered.

Chapter 4 consists of a discussion of the method for obtaining results. The variation of Rayleigh number with parameter values of interest are reported for each of the considered cases. Chapter 5 concludes this investigation of convection in mushy regions under externally imposed uniform magnetic field.

CHAPTER 2

MATHEMATICAL FORMULATIONS

2.1 The model

A binary alloy, undergoing the directional solidification, under the influence of externally imposed uniform magnetic field, at a constant rate V_0 is considered. A distinct mushy layer, which is a mixture of melt and solid dendrites is formed between a lower solidified material and an upper liquid melt. The lower mush-solid interface is kept at eutectic temperature T_E. Let T_∞ be the temperature of liquid far above the mushy layer and $T_\infty > T_L$ where T_L is the liquidus temperature of the alloy. As the alloy solidifies with a given composition, it releases buoyant residual fluid within the mushy layer. A schematic description of this physical system is shown in figure 2.1.

A binary phase diagram is shown in figure 2.2, the left and right extremes correspond to materials in pure form. The point E is the eutectic point. Let C_E and T_E be the composition of the melt at the eutectic point E. When the temperature of the melt is above the liquidus curve, the sample is completely liquid. In the region between the liquidus and the solidus, solid and liquid coexist in equilibrium, with the composition of the liquid phase equal to the liquidus concentration and the composition of the solid phase equal to the solidus concentration at the given temperature. This is the state in the interior of an ideal mushy layer. The regions ACE and BED corresponds to the region of solid and liquid coexist in equilibrium, with the composition of the liquid phase is equal to the liquidus concentration and the composition of solid phase is equal to the solidus concentration at the given temperature. The region ACF represents material of a single phase, in which atoms of one component are incorporated into the lattice of the other to form a solid solution. Below the eutectic temperature T_E , a composite solid forms composed of crystals of both of the end members of the alloy. In an ideal mushy layer, the liquidus is taken to be linear, as shown on the right.

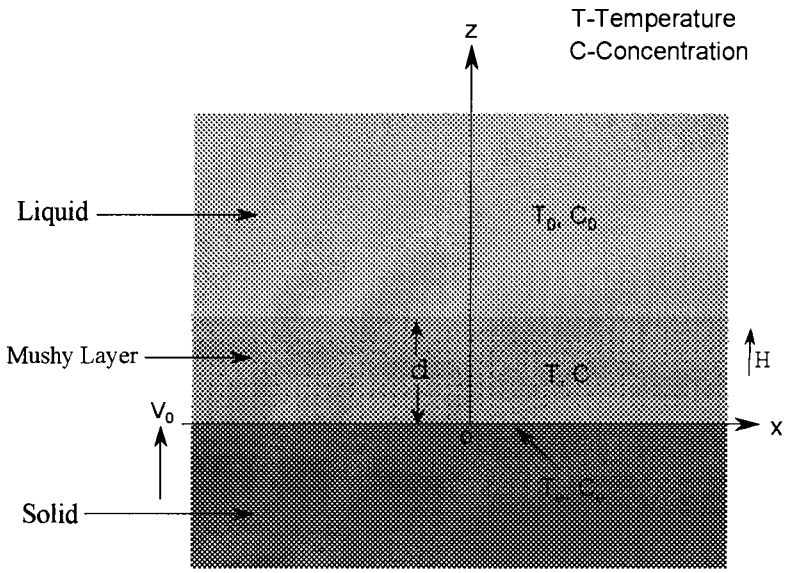

Figure 2.1: The diagram showing the physical system under consideration.

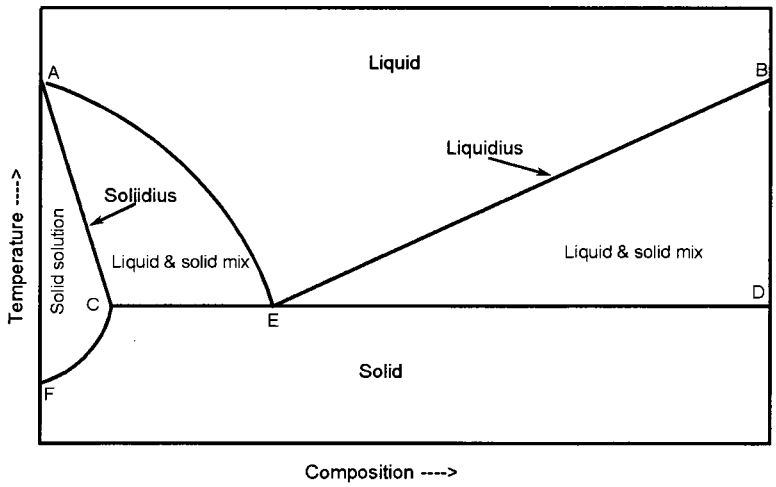

Figure 2.2: The equilibrium phase diagram of a eutectic binary alloy.

We assume that the concentration of the melt C_0 is greater than the eutectic concentration C_E. The concentration of the liquid is related to the temperature in the mush by the liquidus relation (Worster 1991).

$$T = T_L(C) = T_E + \Gamma(C - C_E), \tag{2.1}$$

where Γ is the slope of the liquidus. The density of the fluid is expressed in terms of its temperature T and composition C as

$$\rho_l = \rho_0[1 - \alpha^*(T - T_0) - \beta^*(C - C_0)], \tag{2.2}$$

where α^* and β^* are expansion coefficients for heat and solute, respectively, and ρ_0, T_0, and C_0 are reference values. Using equation (2.1) in (2.2), the equation of state can be written as

$$\rho_l = \rho_0[1 - (\alpha^*\Gamma - \beta^*)(C - C_0)]. \tag{2.3}$$

Many authors took different approaches to the formulation of governing equations. We follow an approach close to Worster (1991, 1992) for the so called ideal mushy layer (Worster 1997). Conservation equations for hydro-magnetic convective flow (Chandrasekhar 1961, Riahi 2000) through Darcy law are derived at the continuum level. When the Oberbeck-Boussinesq approximation is applied, the equation for conservation of mass, momentum, heat and concentration can be written as

$$\nabla . \bar{u} = 0, \tag{2.4}$$

$$\nabla . \bar{H} = 0, \tag{2.5}$$

$$\frac{\upsilon}{\Pi(\hat{\chi})}\bar{u} - \frac{\mu\bar{H}}{4\pi\rho}\cdot\nabla\bar{H} = -\nabla\left(\frac{p}{\rho} + \mu\frac{|H|^2}{8\pi\rho}\right) - \left(\frac{\rho}{\rho_0} - 1\right)g, \tag{2.6}$$

$$\frac{\partial H_i}{\partial t} + \frac{\partial}{\partial x_j}(u_j H_i - u_i H_j) = \eta\nabla^2 H_i, \tag{2.7}$$

$$c_m(\partial_{\bar{t}} - V_0\partial_{\bar{z}})T + c_l\bar{u}\cdot\nabla T = \nabla\cdot(k_m\nabla T) - \mathscr{L}(\partial_{\bar{t}} - V_0\partial_{\bar{z}})\hat{\chi}, \tag{2.8}$$

$$(\partial_{\bar{t}} - V_0\partial_{\bar{z}})[\chi C + (\hat{1} - \hat{\chi})C_s] + \bar{u}\cdot\nabla C \;=\; \nabla\cdot(D_m\nabla C). \tag{2.9}$$

Here p is static pressure, $\mathscr{L}$ is the latent heat of solidification, $\bar{u}$ is the Darcy velocity, $\bar{H}$ is the magnetic field, υ is the dynamic viscosity, Π is the permeability function, $\hat{\chi}$ is liquid volume fraction, ρ is the density, g is the acceleration due to gravity, c_m, $k_m$and D_m are weighted averages of specific heat, heat and molecular mass respectively, $\partial_{\bar{t}}$ and $\partial_{\bar{z}}$ are partial derivatives with respect to $\bar{t}$ and $\bar{z}$.

At the solid-mush interface, $\bar{z} = 0$, the temperature is held at the eutectic temperature and no penetration of fluid into the solid region is possible:

$$T = T_E, \quad \bar{u}\cdot e_z = 0, \tag{2.10}$$

where e_z is the unit vector oriented along the vertical axis.

At the mush-liquid interface, Worster (1986, 1991) introduces two interfacial conditions that express conservation of heat, solute and the continuity of mass flux, temperature and heat flux. These can be expressed as

$$[n\cdot\bar{u}] = 0,\ [p] = 0,\ [T] = 0,\ [n\cdot\nabla T] = 0 \tag{2.11}$$

In one case, we assume that the mush-liquid interface is impermeable, so that,

$$n\cdot\bar{u} = 0 \tag{2.12}$$

Chung and Chen (2000) considered the Amberg-Homsy (1993) model with one modification. Instead of considering the mush-liquid interface to be impermeable, they considered the mush-liquid interface to be permeable so that the vertical velocity gradient is zero.

$$n\cdot\nabla(\bar{u}\cdot n) = 0 \tag{2.13}$$

In (2.13), n is a unit vector normal to the interface and in (2.11), [ ] denotes the jump in the enclosed quantity across the interface. We will consider both cases (2.12) and (2.13) in this study.

2.2 Nondimensional System

The governing equations are dimensionalised by the following scalings. Velocity is scaled by the speed of the solidification front, V_0. Length and time scales are made dimensionless using κ/V_0, κ/V_0^2 respectively. Pressure is scaled by $[(\beta^* - \Gamma\alpha^*)\Delta C \rho_0 g \kappa]/V_0$, Concentration of solute is scaled by $\Delta C = C_0 - C_E$, temperature is scaled by $\Delta T = T_L(C_0) - T_E$. Finally the magnetic field is scaled by $\hbar$.

The non-dimensional form of the basic equations for the hydromagnetic convective flow in mushy layer are given by

$$\nabla \cdot \vec{U} = 0, \tag{2.14}$$

$$\nabla \cdot \vec{H} = 0, \tag{2.15}$$

$$K\vec{U} + \nabla P + R\Theta\hat{k} - \frac{Q}{\tau}\left(\frac{\partial}{\partial z} + \vec{H}\cdot\nabla\right)\vec{H} = 0, \tag{2.16}$$

$$\left(\frac{\partial}{\partial t} - \frac{\partial}{\partial z}\right)\vec{H} + \vec{U}\cdot\vec{H} - \left(\frac{\partial}{\partial z} + \vec{H}\cdot\nabla\right)\vec{U} - \frac{1}{\tau}\nabla^2\vec{H} = 0, \tag{2.17}$$

$$\left(\frac{\partial}{\partial t} - \frac{\partial}{\partial z}\right)[\Theta - S\Phi] + \vec{U}\cdot\Theta - \nabla^2\Theta = 0, \tag{2.18}$$

$$\left(\frac{\partial}{\partial t} - \frac{\partial}{\partial z}\right)[(1-\Phi)\Theta + C\Theta] + \vec{U}\cdot\nabla\Theta = 0, \tag{2.19}$$

where $\vec{U} = U\hat{i} + V\hat{j} + W\hat{k}$ is the volume flux vector per unit area, which is also known as the Darcy velocity vector, U and V are the horizontal components of $\vec{U}$, W is the vertical component of $\vec{U}$, P is the non-dimensional modified pressure, Θ is the non-dimensional temperature, equivalently modified composition, $\Theta = [T - T_L(C_0)]/\triangle T$, also $\Theta = (C - C_0)/\triangle C$, t is the time variable, Φ is the local solid volume fraction, $R = \beta \triangle C g \Pi_0 / V_0 \upsilon$ is the mush Rayleigh number, Π_0 is reference value of permeability of the porous medium, which is assumed to be finite, $K = \Pi_0/\Pi$ is the permeability function of the medium, υ is the kinematic viscosity, β is the expansion co-efficient of solid, $Q = \mu\hbar^2\Pi_0/(4\pi\rho_0\nu\eta)$ is the Chandrasekhar number which represents the strength of externally imposed magnetic field, μ is the magnetic permeability, η is the magnetic diffusivity, $\tau = \kappa/\eta$ is the Roberts number, $\hbar$ is the uniform magnetic field's strength, $S = L/\gamma\triangle T$ is the Stefan number, γ is the specific heat per unit volume, L is the Latent heat of

solidification per unit volume, $C = (C_s - C_0)/\triangle C$ is a concentration ratio, C_s is the composition of the solid phase forming the dendrites. In addition $\hat{i}$, $\hat{j}$ and $\hat{k}$ are unit vectors along X-, Y- and Z- directions, respectively.

The above governing equations are subjected to the following boundary conditions

$$\Theta = -1, \quad W = 0, \quad \vec{H} = \hat{k} \quad at \quad Z = 0, \tag{2.20}$$

$$\Theta = 0, \quad \Phi = 0, \quad W = 0 \quad or \quad \partial_z W = 0, \quad \vec{H} = \hat{k} \quad at \quad Z = \delta. \tag{2.21}$$

Where $\delta = dV_0/\kappa$ is the growth Peclet number representing the dimensionless depth of the mushy layer, d is the thickness of the mushy layer. The non-dimensional boundary conditions (2.21) at the upper boundary correspond to those for an impermeable flat boundary with zero solid fraction, whose temperature is that of the liquidus temperature relevant for the flow a single-mushy layer model (Amberg and Homsy, 1993). In addition, we also used the continuity of the heat flux across the mush-liquid interface to determine a relation for the basic state solution for the temperature.

We use a Kozeny-Carman type of relation for variable permeability (Worster, 1992), as a function of porosity or local liquid fraction,

$$K(x, y, z, t) = \frac{\Pi_0}{\Pi(\Phi)}. \tag{2.22}$$

The Permeability Π is derived from

$$\Pi(\Phi) = (1 - \Phi(x, y, z, t))^n.$$

Hence the Permeability function is given by

$$K = (1 - \Phi)^{-n}. \tag{2.23}$$

In the above permeability function, n = 0 represents the case of constant permeability in

which there is no coupling between permeability and porosity and is known as the case of passive mushy layer. Also $n = 3$ in equation (2.22) represents the case of variable permeability which is known as the case of reactive mushy layer. Hence in $K = (1-\Phi)^{-3}$, K increases as Φ increases, which is physically realistic. These two relations for K has been used by many authors (Worster 1992, Amberg and Homsy 1993, Emms and Fowler 1994, Okhuysen and Riahi 2008a) in similar studies.

CHAPTER 3

PERTURBATION ANALYSIS

Here we employ a similar approach to the one of Okhuysen and Riahi (2008), if the constraint of analytical solutions is removed and the use of one-dimensional numerical integration is accepted, then the linear stability of the governing system may be studied for fixed parameter values.

3.1 Steady Basic State and Perturbation Systems

The basic state is considered to be motionless and the corresponding quantities are designated by subscript ' b ' and are assumed to be functions of Z.

$$\Theta = \theta_b(Z) + \varepsilon\,\theta(x, y, z, t), \tag{3.1}$$

$$\Phi = \phi_b(Z) + \varepsilon\,\phi(x, y, z, t), \tag{3.2}$$

$$\vec{U} = \vec{0} + \varepsilon\,\vec{u}(x, y, z, t), \tag{3.3}$$

$$P = p_b(z) + \varepsilon\,p(x, y, z, t), \tag{3.4}$$

$$\vec{K} = K_b(\phi_b) + \varepsilon\,K(x, y, z, t), \tag{3.5}$$

$$\vec{H} = \hat{k} + \varepsilon\,\vec{h}(x, y, z, t), \tag{3.6}$$

where $\varepsilon(\varepsilon<<1)$ is the perturbation parameter and the perturbed quantities can vary with respect to spatial and time variables. θ, ϕ, $\vec{u}$, p, K and $\vec{h}$ are the perturbed quantities for the corresponding dependent variables. Using equation (3.1) - (3.6) in (2.14) - (2.19) and the boundary conditions (2.20) - (2.21) and setting all perturbation quantities to be zero, we find the following steady basic-state system of equations.

$$\frac{d^2\theta_b}{dz^2}+\frac{d\theta_b}{dz} = S\frac{d\phi_b}{dz}, \tag{3.7}$$

$$(1-\phi_b)\frac{d\theta_b}{dz} = (\theta_b - C)\frac{d\phi_b}{dz}, \tag{3.8}$$

$$\frac{dp_b}{dz} = -R\,\theta_b. \tag{3.9}$$

The corresponding boundary conditions are as follows

$$\theta_b = -1 \quad at \quad z=0, \tag{3.10}$$

$$\theta_b = \phi_b = 0 \quad at \quad z=\delta. \tag{3.11}$$

In order to solve (3.7) - (3.9) along with the boundary conditions (3.10) - (3.11), we follow Okhuysen and Riahi (2008). We integrate the heat and solute equations once, apply the boundary conditions and then substitute the expression for ϕ_b into the integrated form of the heat equation, integrate and apply the boundary conditions again to determine the basic state solutions. We also used a boundary condition at the top boundary $d\theta_b/dz = \theta_\infty$ (Worster, 1991, 1992), where $\theta_\infty = [T_\infty - T_L(C_0)]/\triangle T$ is the non-dimensional far-field temperature. Using this boundary condition, we find the following inverse relation for basic-state temperature,

$$z(\theta_b) = \frac{A-C}{A-B}\ln\left[\frac{1+A}{A-\theta_b}\right]+\frac{C-B}{A-B}\ln\left[\frac{1+B}{B-\theta_b}\right], \tag{3.12}$$

where A and B are the roots of the equation $\theta_b^2-(S+C+\theta_\infty)\theta_b+C\theta_\infty=0$. The values of A and B in terms of S, C and θ_∞ are given by the following equations

$$A = \frac{S+C+\theta_\infty+\sqrt{(S+C+\theta_\infty)^2-4C\theta_\infty}}{2}, \tag{3.13}$$

$$B = \frac{S+C+\theta_\infty-\sqrt{(S+C+\theta_\infty)^2-4C\theta_\infty}}{2}. \tag{3.14}$$

The basic-state solid fraction and pressure are given by

$$\phi_b = \frac{\theta_b}{\theta_b - C}, \tag{3.15}$$

$$p_b = -R\int \theta_b dz + P_0, \tag{3.16}$$

where P_0 is a constant.

To determine the thickness of the mushy layer δ, we use the remaining boundary condition in (3.11) for the basic-state temperature at the upper boundary by replacing θ_b and z in (3.12) with 0 and δ, respectively. Thus the following expression for δ is obtained as function of the parameters S, C and θ_∞

$$\delta = \frac{A-C}{A-B}\ln\left[\frac{1+A}{A}\right] + \frac{C-B}{A-B}\ln\left[\frac{1+B}{B}\right]. \tag{3.17}$$

Using (3.5) in (2.23), we find a relation for the basic-state permeability function as

$$K_b = (1-\Phi_b)^{-n}. \tag{3.18}$$

3.2 Linear Perturbation System

We find the following linear perturbation system and the corresponding boundary conditions that will be needed for further analysis

$$K_b\vec{u}+\nabla p+R\theta\hat{k}-\frac{Q}{\tau}\frac{\partial\vec{h}}{\partial z} = 0, \quad (3.19)$$

$$\left(\frac{\partial}{\partial t}-\frac{\partial}{\partial z}\right)\vec{h}+\frac{\partial\vec{u}}{\partial z}-\frac{1}{\tau}\nabla^2\vec{h} = 0, \quad (3.20)$$

$$\nabla\cdot\vec{u} = 0, \quad (3.21)$$

$$\nabla\cdot\vec{h} = 0, \quad (3.22)$$

$$\left(\frac{\partial}{\partial t}-\frac{\partial}{\partial z}-\nabla^2\right)\theta-S\left(\frac{\partial}{\partial t}-\frac{\partial}{\partial z}\right)\phi+w\frac{d\theta_b}{dz} = 0, \quad (3.23)$$

$$\left[(1-\phi_b)\left(\frac{\partial}{\partial t}-\frac{\partial}{\partial z}\right)+\frac{d\phi_b}{dz}\right]\theta-(\theta_b-C)\left(\frac{\partial}{\partial t}-\frac{\partial}{\partial z}\right)\phi+\frac{d\theta_b}{dz}(\phi+w) = 0. \quad (3.24)$$

The boundary conditions are given by

$$\theta = w=h_3=0 \quad at \quad z=0, \quad (3.25)$$

$$\theta = w \quad or \quad \partial_z w=0, \phi=h_3=0 \quad at \quad z=\delta, \quad (3.26)$$

where h_3 is the vertical component of induced magnetic field $\vec{h}$.

The perturbation equations and the boundary conditions are obtained by taking the z-component of the double-curl of equation (3.19), z-component of equation(3.20) and using equations (3.21) and (3.22), we obtain the following coupled system.

$$\nabla^2 w+\frac{1}{K_b}\cdot\frac{dK_b}{dz}\cdot\frac{\partial w}{\partial z}+\frac{R}{K_b}\triangle_2\theta-\frac{Q}{\tau K_b}\cdot\frac{\partial}{\partial z}\cdot\nabla^2 h_3 = 0, \quad (3.27)$$

$$\left(\frac{\partial}{\partial t}-\frac{\partial}{\partial z}\right)h_3-\frac{\partial w}{\partial z}-\frac{1}{\tau}\nabla^2 h_3 = 0, \quad (3.28)$$

$$\left(\frac{\partial}{\partial t}-\frac{\partial}{\partial z}-\nabla^2\right)\theta-S\left(\frac{\partial}{\partial t}-\frac{\partial}{\partial z}\right)\phi+w\frac{d\theta_b}{dz} = 0, \quad (3.29)$$

$$\left[(1-\phi_b)\left(\frac{\partial}{\partial t}-\frac{\partial}{\partial z}\right)+\frac{d\phi_b}{dz}\right]\theta-(\theta_b-C)\left(\frac{\partial}{\partial t}-\frac{\partial}{\partial z}\right)\phi+\frac{d\theta_b}{dz}(\phi+w) \;=\; 0, \quad (3.30)$$

where ∇^2 and $\triangle_2$,respectively, 3D and 2D laplacian, and the boundary conditions are

$$\theta \;=\; w=h_3=0 \quad at \quad z=0, \quad (3.31)$$

$$\theta \;=\; w \quad or \quad \partial_z w=0, \phi=h_3=0 \quad at \quad z=\delta. \quad (3.32)$$

Since the coefficients in (3.27) - (3.30) are functions of z only, we use normal mode approach (Chandrasekhar 1961). The perturbations are expressed in terms of a set of normal modes in the form of two dimensional waves.

$$(w,\, \theta,\, \phi,\, h_3)=[\widetilde{w}(z),\, \widetilde{\theta}(z),\, \widetilde{\phi}(z),\, \widetilde{h_3}(z)]\cdot exp(ikx+\sigma t), \quad (3.33)$$

where k is the wave number of the disturbance, i is the imaginary unit $\left(i=\sqrt{-1}\right)$, x is the horizontal variable, t is the time variable and σ is the growth rate of the disturbance, for the onset of stationary solution we seek $\sigma=0$. Using (3.33) in (3.27) - (3.32). These give rise to the following linearized equations and boundary conditions in which the variables w, θ, ϕ, h_3 represent the disturbance amplitudes.

In mushy region, $0<z<\delta$, the disturbance equations take form

$$(D^2-k^2)\widetilde{w}+\frac{1}{K_b}\cdot\frac{dK_b}{dz}\cdot\frac{\partial\widetilde{w}}{\partial z}-\frac{Rk^2}{K_b}\widetilde{\theta}-\frac{Q}{\tau K_b}\cdot D(D^2-k^2)\widetilde{h_3} \;=\; 0, \quad (3.34)$$

$$(\sigma-D)\widetilde{h_3}-D\widetilde{w}-\frac{1}{\tau}(D^2-k^2)\widetilde{h_3} \;=\; 0, \quad (3.35)$$

$$(\sigma-D-D^2+k^2)\widetilde{\theta}-S(\sigma-D)\widetilde{\phi}+wD\theta_b \;=\; 0, \quad (3.36)$$

$$[(1-\phi_b)(\sigma-D)+D\phi_b]\,\widetilde{\theta}-(\theta_b-C)(\sigma-D)\,\widetilde{\phi}+D\theta_b\left(\widetilde{\phi}+\widetilde{w}\right) \;=\; 0. \quad (3.37)$$

The corresponding boundary conditions applied to dependent variables are

$$\widetilde{\theta} = \widetilde{w} = \widetilde{h_3} = 0 \quad at \quad z = 0, \tag{3.38}$$

$$\widetilde{\theta} = \widetilde{w} \quad or \quad \partial_z \widetilde{w} = 0, \widetilde{\phi} = \widetilde{h_3} = 0 \quad at \quad z = \delta. \tag{3.39}$$

3.3 Computational Procedure

The analytical solution obtained in equation (3.12) gives z in terms of basic-state temperature, θ_b. We use Muller's method (Cheney and Kincaid, 2008) to obtain the basic-state temperature from this equation without actually inverting it. The basic-state solid volume fraction, ϕ_b is then computed from equation (3.15) using θ_b obtained above. Using equation (3.17), we compute the thickness of the mushy layer.

To analyze the marginal stability numerically, we first convert the linear system involving ordinary differential equations (ODE) and boundary conditions given by equations (3.34) - (3.39) to a linear system involving simple ODEs and corresponding boundary conditions. Multiple shooting technique (Cheney and Kincaid, 2008) is used to solve this ODE system. Starting at z = 0, for a fixed wave number, and Rayleigh number, we integrate the ODEs using an efficient fourth order Runge-Kutta algorithm (Cheney and Kincaid, 2008) for four different initial conditions until we reach $z = \delta$. Then at $z = \delta$, we apply the boundary conditions and check the value of Det = Det (k, R: Q, θ_∞, τ, S, C). We iterate over R and repeat the same procedure until Det ≈ 0. This procedure was repeated, until we get a pair of wave number and Rayleigh number (k, R). The minimum value of the eigenvalue R_c with respect to k_c is then determined from the marginally stable state values for different $k_c s$. At a minimum point on the marginal stability curve, which is the least upper bound on a stable flow regime, above which instabilities will manifest. Then the linear solutions at that critical wave number and Rayleigh number are determined. Marginal stability graphs are obtained for different cases of magnetic field, far-field temperature, magnetic field gradient and variable permeability parameter.

The strength of externally imposed magnetic field represented by a non dimensional Chandrasekhar number, Q is chosen as 0.01, 1.0 and 3.0 to represent the cases of weak, moderate and

strong magnetic field (Riahi 2000). For the case of non-magnetic field, we use $Q = 0$. Also the Roberts number is set as 0.0001 (Vives and Perry, 1987). The effects of Roberts number on the convective instabilities during steady solidification of binary alloys were reported as very little or no effect (Riahi, 2000). In the present study we also notice very little effect of variation of the Roberts number, τ, on the solution.

CHAPTER 4

RESULTS

Here we consider a particular set of parameter values, namely, the concentration ratio, C = 9.0, Stefan number, S = 3.2 and far-field temperature, θ_∞= 0.1, 0.2, 0.3. These values are taken from relevant experimental studies concerning the solidification of ammonium chloride solution (Tait and Jaupart, 1992, Chung and Chen 2005). The computed thickness, δ of the mushy layer from equation(3.17) are 1.9894, 1.5239 and 1.2687 for far-field temperature 0.1, 0.2 and 0.3 respectively. It is observed that thickness of the mushy layer decreases as the far-field temperature increases. This is due to the fact that, increasing far-field temperature transfer more heat flux from liquid region and hence reduces the thickness of the mushy layer (Worster 1992, Okhuysen 2005).

As a way to validate our present computational code, we first considered the case in the absence of the magnetic field and generated data for particular values of the parameters C, S and θ_∞ similar to those used in Okhuysen (2005). We found very good qualitative and quantitative agreements between our results for the critical values of the Rayleigh number and the wave number and those in Okhuysen (2005).

Nature of mushy layer	Okhuysen(2005)	Present study
Passive mushy layer	k_c= 11.183 R_c=120.25	k_c= 11.183 R_c=120.1025
Reactive mushy layer	k_c= 11.217 R_c=157.89	k_c= 11.217 R_c=157.324

4.1 Passive Mushy layer

We now focus on a mushy layer in which the permeability function $K = 1$(i.e. n = 0 in eq(2.23)), there is no coupling between permeability and porosity. For a two dimensional convection, the parameter values were selected from the available experimental studies concerning the solidification of binary alloys. In order to make the model realistic, the values of far-field temperature

were taken from Tait and Jaupart (1992b), and we select the value of concentration ratio C = 9.0 and Stefan number S = 3.2 from experimental studies of Chen and Chen (1995). Under the case of passive mushy layer, two explicit cases for impermeable and permeable mush-liquid interface were examined. The eigenvalue relationship $E(R, k, C, S, \theta_\infty, Q, \tau, \sigma) = 0$, then specifies a marginal-stability curve of R_c v/s k_c for each choice of dimensionless parameters such as Q, θ_∞ and τ. The system is unstable in the region above each curve and is stable below the curve.

4.1.1 Impermeable mush-liquid interface

Here the top boundary is assumed to be impermeable, ie there is no outflow at the mush-liquid interface. The first illustrative example of marginal stability curve is displayed in fig (4.1), which shows the effect of far-field temperature, θ_∞ on marginal stability for weak magnetic field, Q = 0.01. The system is convectively unstable to the disturbances of wave number k_c whenever the Rayleigh number is greater than the value R_c given by the marginal stability curve. The striking property of this marginal curve is that the critical Rayleigh number, R_c and wave number, k_c increase with increasing far-field temperature, θ_∞. This result agrees with result obtained by Worster (1992). The increasing critical Rayleigh number indicates that the mushy layer is more stable, and the increasing wave number reflects the fact that instability manifest at shorter wave length. This behavior is expected as the mushy layer gets thinner with increasing far-field temperature. The critical pair (k_c, R_c) for $\theta_\infty = 0.1$ is (1.7, 18.6), which agrees qualitatively with the value obtained for the case of no magnetic field by Okhuysen (2005).

For the case of moderate magnetic field, the value of Q is taken as 1.0. Figure (4.2) indicates the effect of Q on critical Rayleigh number for different values of far-field temperature θ_∞ = 0.1, 0.2 and 0.3. It can be seen that the far-field temperature is stabilizing for the case of moderate field in the sense that the critical Rayleigh number increases with increasing far-field temperature. Also, the critical pair for Q = 1.0 and $\theta_\infty = 0.1$ is (2.0, 26.5), which is qualitatively higher than in the case of weak magnetic field. The same qualitative result was found to be valid for the case of strong magnetic field(Q = 3.0).

Figure (4.3) shows the effect of magnetic field on the onset of motion, the critical Rayleigh

number increases with increasing Q. It can be seen that magnetic field has notable stabilizing effect on the onset of convective motion in the sense that the value of the critical Rayleigh number increases with the strength of the magnetic field.

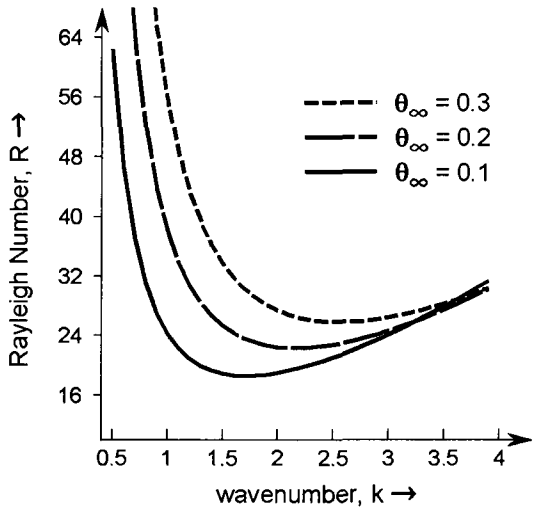

Figure 4.1: Effect of far-field temperature on marginal stability for the case of weak magnetic field $Q = 0.01$

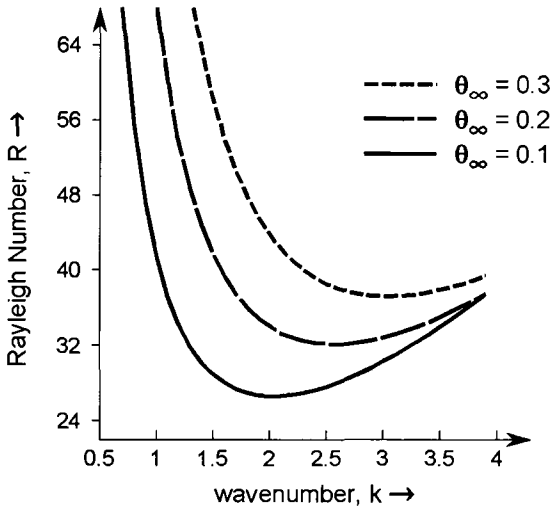

Figure 4.2: Marginal stability graph showing the effect of far-field temperature for the case of moderate magnetic field $Q = 1.0$.

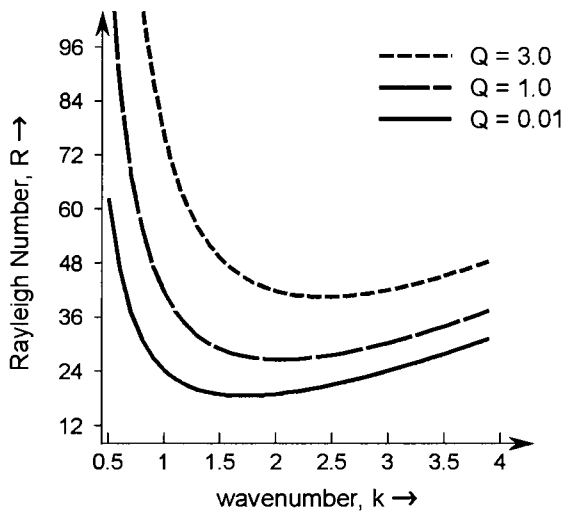

Figure 4.3: Effect of magnetic field on marginal stability for $\theta_\infty = 0.1$.

4.1.2 Permeable mush-liquid interface

Here we consider passive mushy layer with out flow at the top. The condition ($\partial w/\partial z = 0$) of permeable mush-liquid interface, which is much closer to the experimental condition than a non-permeable $W = 0$ condition at such surface, was used first by Chung and Chen (2000) in their theoretical study of directional solidification. The present permeable interface condition can be derived using the constant pressure condition across mush-liquid interface (Okhuysen and Riahi 2008).

Figure (4.4) shows the effect of far-field temperature for moderate magnetic field ($Q = 1.0$) on the marginal stability. The critical Rayleigh number and wave number increases with increasing far-field temperature. The computed values of the critical pair (k_c,R_c) are (1.5, 20.6807), (1.9, 23.5612) and (2.3, 26.4707) for θ_∞= 0.1, 0.2 and 0.3 respectively. It is seen from this figure that the effect of the far-field temperature is stabilizing in the sense that R_c increases with the far-field temperature for the case of moderate magnetic field. The same qualitative result was found to be valid for the cases of weak ($Q = 0.01$) and strong fields ($Q = 5.0$).

Figure (4.5) shows the stabilizing effect of externally imposed magnetic field, which can be weak ($Q = 0.001$), moderate ($Q = 1$) or strong ($Q = 5$), on the marginal stability curve for θ_∞= 0.1. The critical Rayleigh number and wave number increase with increasing Q. The point (k_c , R_c) on the curve shifts to the right side as the value of Q increases. Hence externally imposed strong uniform magnetic field has stabilizing effect on solidification.

Comparison of the marginal stability curves for permeable and impermeable mush-liquid interface is shown in Figure (4.6). It is clear that the present permeable interface condition destabilizes the convection by reducing the critical Rayleigh number. Figure (4.7) depicts the variation of the vertical velocity with respect to the permeable and the impermeable mush-liquid interfaces. The result presented in this figure makes it clear that the vertical velocity component is nonzero at the top of mushy layer for the permeable mush-liquid interface condition whereas it is zero for the impermeable mush-liquid interface condition.

The perturbed vertical velocity for the case of moderate magnetic field ($Q = 1.0$) and θ_∞= 0.1 is depicted in Figure (4.8) as function of x and z. It is seen that the peak values of the vertical

velocity increases with z. Figure (4.9), shows the effect of far-field temperature on the vertical velocity for the case of moderate magnetic field, i.e., Q = 1.0. It is clear that the maximum of the vertical velocity occurs around the middle of mushy layer. The computed values of the vertical velocity are higher for smaller far-filed temperatures as seen from the graph. This result is consistent with the stabilizing effect of the far-field temperature.

A three dimensional plot of perturbed solid volume fraction for the case of moderate magnetic field and θ_∞= 0.1 is shown in Figure (4.10). The large values of the solid fraction with positive and negative signs shown near the bottom of the layer at different horizontal locations indicates, in particular, tendency for chimney formation at different locations near lower boundary as far as the linear theory is concerned. The variation in the solid volume fraction towards the bottom of the layer, which is more prominent than at the top region, also was found to hold qualitatively for different values of Q and other parameters.

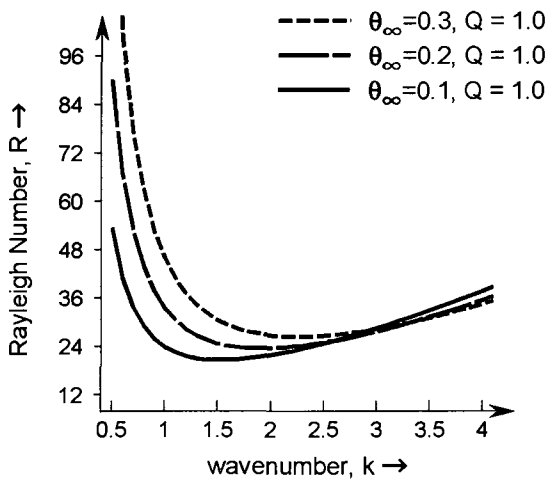

Figure 4.4: Marginal stability graph depicting the effect of far-field temperature for moderate magnetic field $Q = 1.0$.

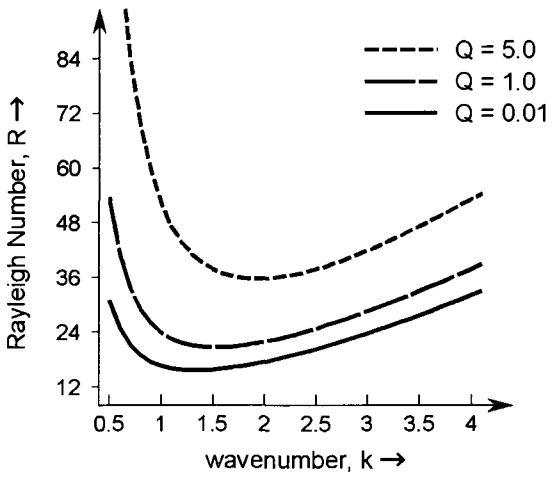

Figure 4.5: Marginal stability graph showing the effect of externally imposed uniform magnetic field for $\theta_\infty = 0.1$.

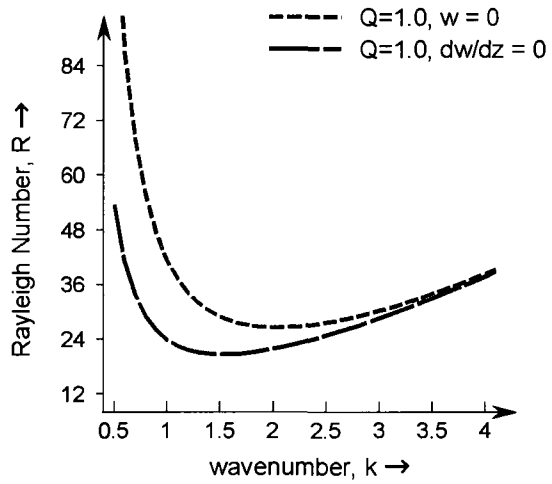

Figure 4.6: Marginal stability graph showing the comparison of impermeable and permeable mush-liquid interface for $Q = 1.0$ and $\theta_\infty = 0.1$.

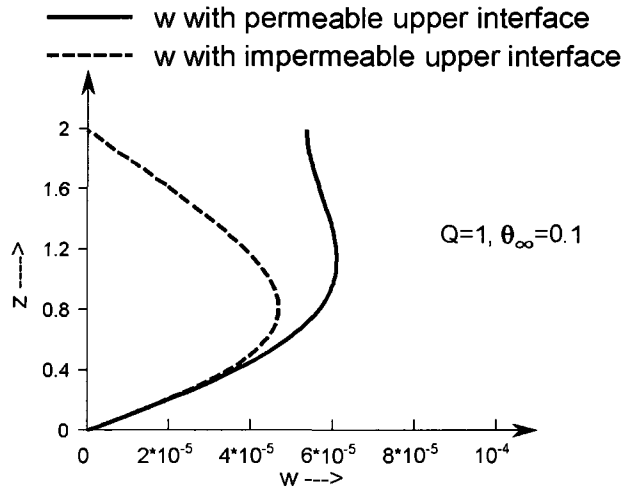

Figure 4.7: Graph of perturbed vertical velocity for impermeable and permeable mush-liquid interface, $Q = 1.0$ and $\theta_\infty = 0.1$.

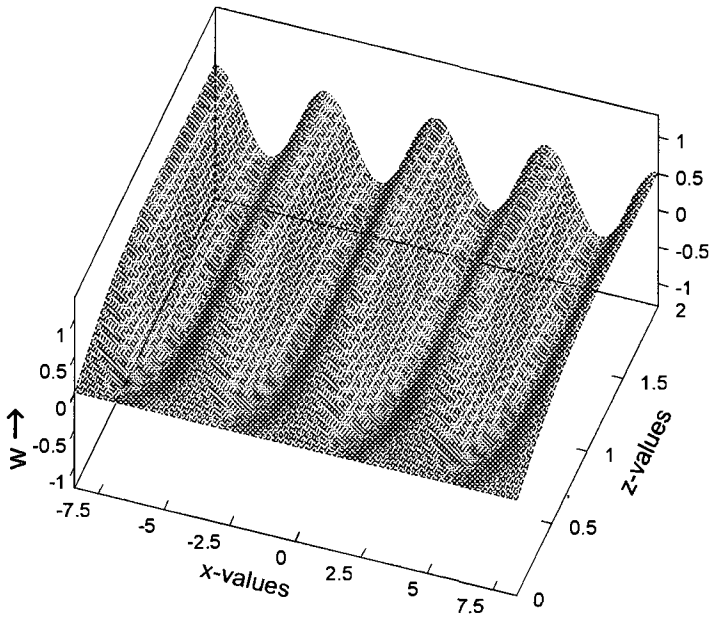

Figure 4.8: 3D plot of perturbed vertical velocity for $Q = 1.0$ and $\theta_\infty = 0.1$.

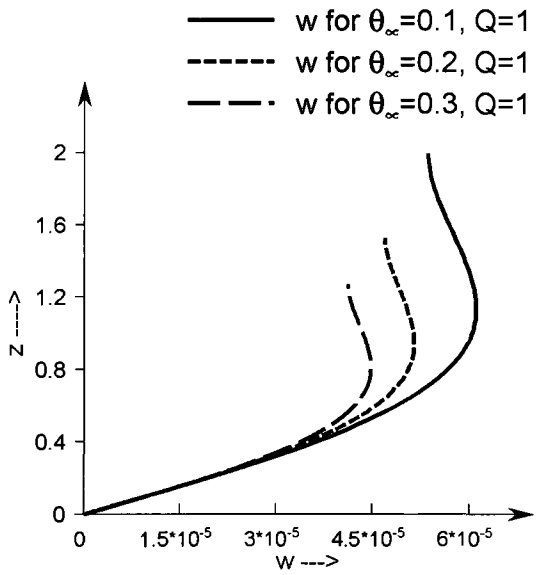

Figure 4.9: Effect of far-field temperature on perturbed vertical velocity for $Q = 1.0$.

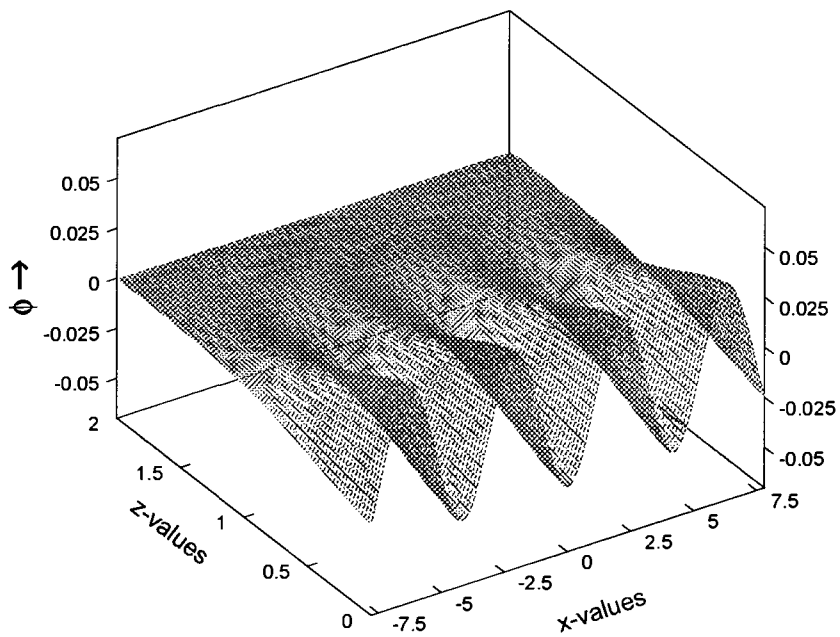

Figure 4.10: 3D graph of perturbed solid volume fraction for $Q = 1.0$ and $\theta_\infty = 0.1$.

4.2 Reactive Mushy layer

The nature and stability of the mushy layer depends on the internal structure of the mushy layer, particularly on its permeability. Here we assume the permeability of the mushy layer is tied to porosity by $K = 1/(1-\phi)^3$(Worster 1992), which can be obtained by selecting the value of n as 3 in equation(2.23). Many researchers used different forms of permeability relations, the present form of K, also known as the Kozeny-Carmen relation, seems to be physically realistic because permeability increases with increasing liquid fraction. With the above permeability function, the linear stability of the mushy layer is investigated for different cases of magnetic field and fixed parameter values.

The Kozeny-Carmen type relation that we used between permeability and the solid fraction with $n = 3$ within the mushy layer is closer to the one in the actual experimental studies than any other relation used by other authors in related theoretical studies.

4.2.1 Impermeable mush-liquid interface

A reactive mushy layer with no out flow at the top is being considered here in the marginal stability analysis. The effect of far-field temperature on the marginal stability for the case moderate magnetic field is depicted in Figure (4.11). It is found that the far-field temperature has stabilizing effect on the solidification. This result is in consistent agreement with previous case of constant permeability also. The stabilizing effect of magnetic field for reactive mushy layer is observed in Figure (4.12) as critical pair (k_c, R_c) for magnetic case shift upwards compared to non-magnetic case.

Marginal stability curve showing the effect of permeability in the case of moderate magnetic field in displayed in Figure (4.13) which demonstrates that reactive mushy layer is more stable than the passive mushy layer.

For the present case of reactive mushy layer with no out flow at the top, the marginal stability graph showing the effect of externally imposed uniform magnetic field is depicted in Figure (4.14). Again critical Rayleigh number and wave number increases when the strength of magnetic field in vertical direction is increased. Figure (4.15) shows the effect of externally imposed

uniform magnetic field on perturbed vertical velocity for the case of variable permeability. This figure reveals that strong magnetic field has more stabilizing effect on the solidification in the sense that it decreases the unwanted convection (Vives and Perry, 1987). For the same magnetic field, the convection in reactive mushy layer is more than the convection with passive mushy layer as displayed in Figure (4.16).

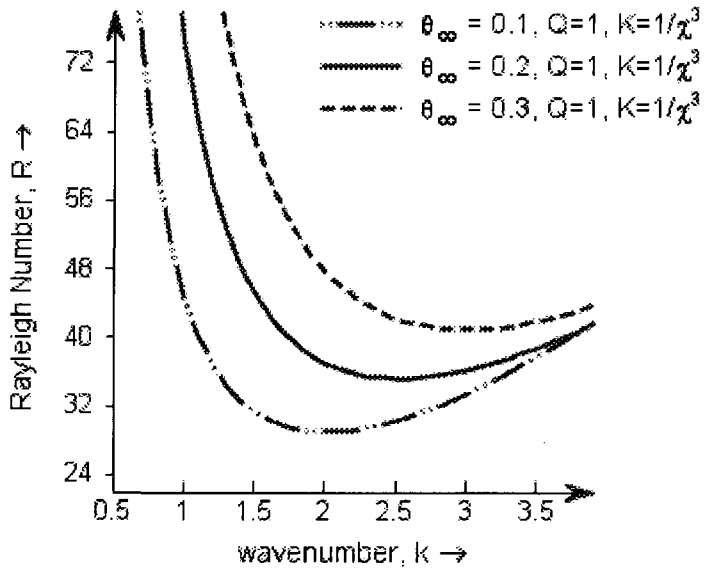

Figure 4.11: Marginal stability graph indicating the effect of far-field temperature for $Q = 1.0$.

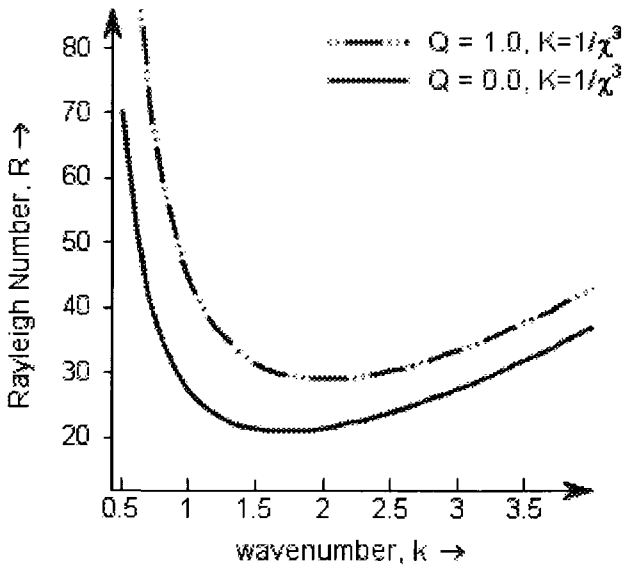

Figure 4.12: Effect of magnetic field on marginal stability for reactive mushy layer for $\theta_\infty = 0.1$.

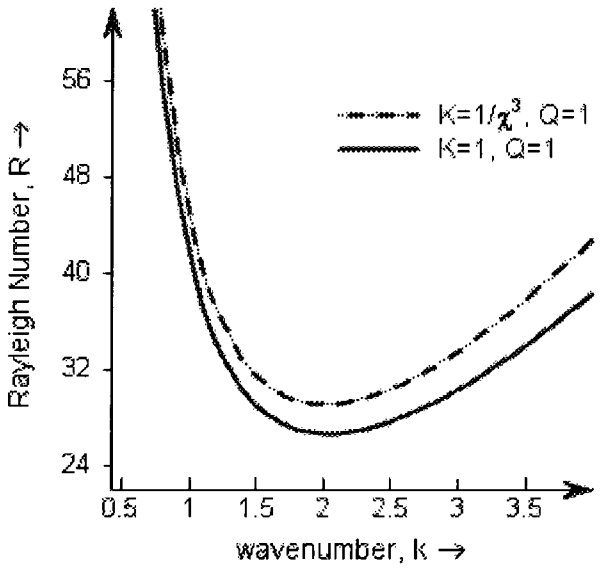

Figure 4.13: Effect of permeability on marginal stability for $Q = 1.0$ and $\theta_\infty = 0.1$.

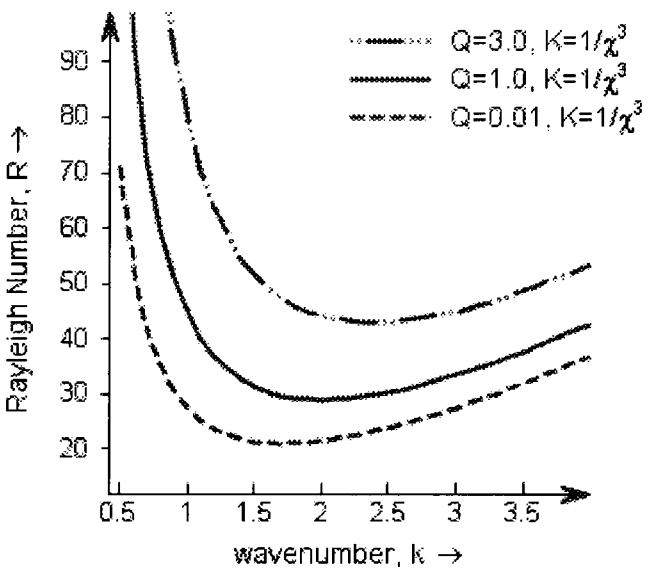

Figure 4.14: Marginal stability graph showing the effect of magnetic field for reactive mushy layer and $\theta_\infty = 0.1$.

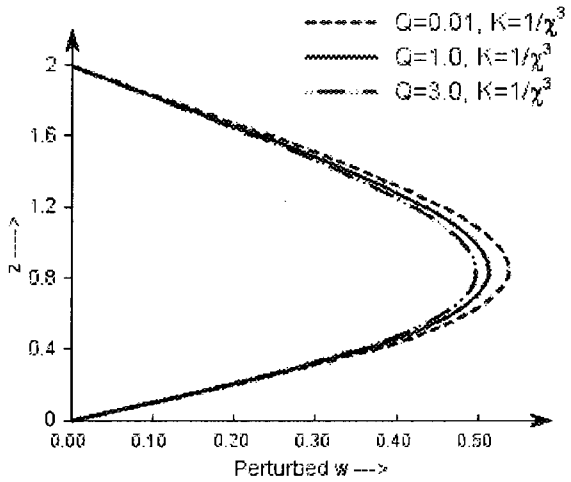
Q=0.01, K=1/χ³
Q=1.0, K=1/χ³
Q=3.0, K=1/χ³
2
1.6
1.2
0.8
0.4
0
z --->
0.00
0.10
0.20
0.30
0.40
0.50
Perturbed w --->
Q=1, K=1
Q=1, K=1/χ³
2.4
2
1.6
1.2
0.8
0.4
0
z --->
0.000
0.125
0.250
0.375
0.500
perturbed w --->
Figure 4.15: Effect of magnetic field on perturbed vertical velocity for reactive mushy layer and θ_∞ = 0.1.
Figure 4.16: Effect of permeability on perturbed vertical velocity for Q = 1.0 and θ_∞ = 0.1.

4.2.2 Permeable mush-liquid interface

In contrast to previous cases, here we treat the mushy layer as a reacting porous medium whose permeability varies as the solid dendrites grow or dissolve within it. We shall discover how the externally impressed uniform magnetic field affects the convection and also the local solid fraction within the mushy layer and draw conclusions regarding the way in which chimney formation can be controlled. The present case of variable permeability and permeable interface condition is more closer to the relevant experimental studies concerning the solidification of binary alloys under externally imposed magnetic field.

The effect of far-field temperature on marginal stability for the case of moderate magnetic field ($Q = 1.0$) is depicted in figure 4.17. The critical Rayleigh number and critical wave number increases with increasing far-field temperature. This indicates that mushy layer is more stable. Increasing wave number indicates that the instability propagates with shorter wave length. The computed values of critical Rayleigh number is much higher compare to the previous interface conditions.

Presence of externally imposed magnetic field in vertical direction with uniform strength is stabilizing in the case of strong field, or is ineffective in the case of weak field, is depicted in figure 4.18. The computed value of critical pair (k_c, R_c) for $Q = 1.0$ and $\theta_\infty = 0.1$ is (1.5, 22.4791). The critical Rayleigh number and critical wave number increases with increasing magnetic field. The system is unstable in the region above each curve and is stable below the curve.

Figure 4.19 indicates the destabilizing effect of permeable mush-liquid interface condition. The critical Rayleigh number is low in the present case of permeable mush-liquid interface condition compare to the case of impermeable mush-liquid interface condition. Even though the permeable interface condition is destabilizing but physically it is realistic.

Effect of externally imposed uniform magnetic field on perturbed vertical velocity component is shown in the figure 4.20. Convection in mushy layer decreases with increasing magnetic field. This interesting result suggests an important operational procedure for possible weakening of convection. Figure 4.21 depicts the variation of the vertical velocity with respect to the permeable and the impermeable mush-liquid interfaces. The result presented in this figure makes it clear

that the vertical velocity component is nonzero at the top of mushy layer for the permeable mush-liquid interface condition whereas it is zero for the impermeable mush-liquid interface condition.

A three dimensional plot of perturbed solid volume fraction for the case of moderate magnetic field and $\theta_\infty = 0.1$ is shown in Figure 4.22. For this case, there is a substantial decrease in the solid fraction in the interior of the mushy layer in regions of up flow which indicates a tendency to form chimneys.

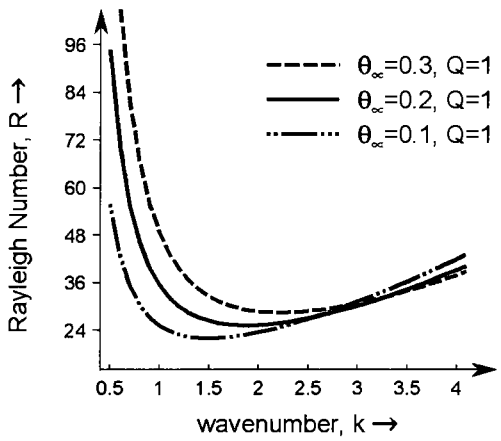

Figure 4.17: Effect of far-field temperature on marginal stability for the case of moderate magnetic field, $Q = 1.0$ and $\theta_\infty = 0.1$.

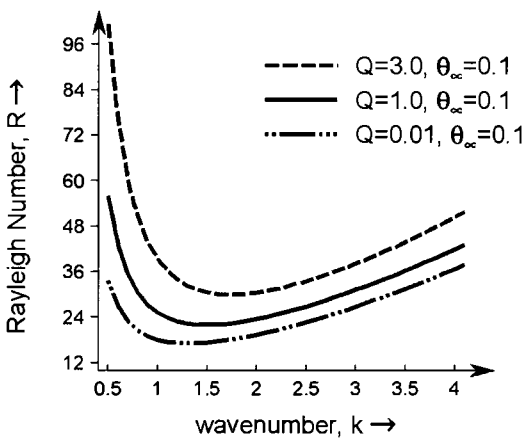

Figure 4.18: Marginal stability graph indicating the effect of magnetic field for $\theta_\infty = 0.1$.

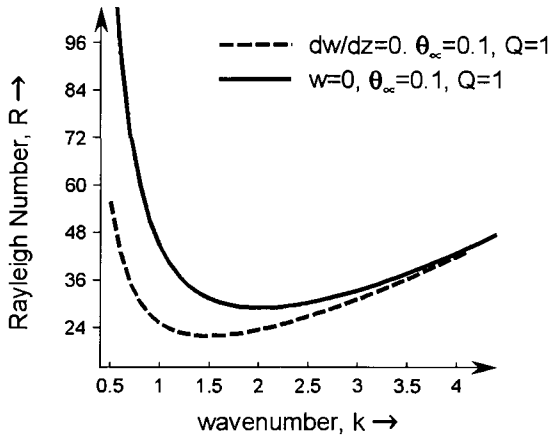

Figure 4.19: Effect of interface condition on marginal stability for the case of moderate magnetic field, $Q = 1.0$ and $\theta_\infty = 0.1$.

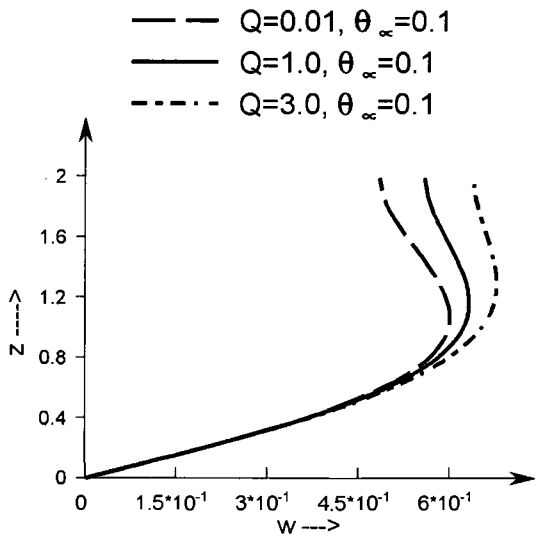

Figure 4.20: Effect of magnetic field on perturbed vertical velocity component for $\theta_\infty = 0.1$.

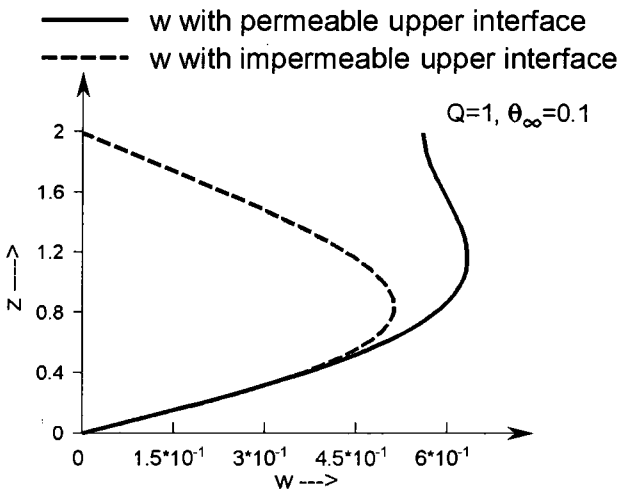

Figure 4.21: Graph of perturbed vertical velocity for impermeable and permeable mush-liquid interface for $Q = 1.0$ and $\theta_\infty = 0.1$.

Figure 4.22: 3D plot showing the variations of perturbed local solid volume fraction for $Q = 1.0$ and $\theta_\infty = 0.1$.

CHAPTER 5

CONCLUSIONS AND SCOPE FOR FUTURE STUDY

Here, we investigated the problem of linear convective stability analysis in a mushy layer under externally imposed uniform magnetic field. Both cases of impermeable and permeable mush-liquid interface coupled with constant and variable permeability were studied. We obtain solutions to linear problem using multiple shooting techniques for the interface conditions and the parameters that we selected from available experiments . We analyze the effect of strength of magnetic field (represented by nondimensional Chandrasekhar number) and far-field temperature on the marginal stability. Our linear stability analysis and the corresponding numerical results indicate the presence of mushy layer mode, which is primarily responsible for the formation of the chimneys. The results of the perturbation analysis and computations are as follows.

(1) permeable mush-liquid interface condition for passive mushy layer destabilizes the convection as the critical Rayleigh number is low compared to the case of impermeable mush-liquid interface.

(2) Far-field temperature has stabilizing effect in the sense that the critical Rayleigh number increases with increasing far-field temperature. This result for the flow stability is in some partial agreement with the results of those previous related studies of several researchers.

(3) Externally imposed strong uniform magnetic field in vertical direction has stabilizing effect on the solidification compared to the case of weak or moderate magnetic field since the critical Rayleigh number is much higher compare to the other two cases.

(4) Our computational results indicates that the Robert's number, τ, has very little or no effect on critical Rayleigh number for all the far-field temperature that we considered.

(5) The convection in the chimneys can be reduced or weakened by maintaining sufficiently high far-field temperature and strong magnetic field. This result suggests an important industrial procedure for possible elimination of freckle formation tendency.

(6) We also investigated numerically the present eigenvalue problem for cases of perturbation's growth rate with non-zero imaginary part in order to explore the possibility for the presence of an oscillatory mode of convection, but we were unsuccessful for the present set of parameter values that we considered in this thesis.

Future studies include additional effects due to externally imposed rotational constraints, due to a vertical rotation or a high gravity environment, extension to weakly nonlinear modeling in presence of externally imposed magnetic field and/or externally imposed rotational constraint. Also, future studies for extension of the present model to the cases of two-layer system with or without inclusion of a magnetic field or a rotational constraints, can all be very important in order to establish a very reliable mathematical model which can be used for flow control cases in material processing and crystal growth industries.

Also a complete stability investigation, which require full numerical computation, without using perturbation approach, which requires extensive work and will be a topic for future study.

REFERENCES

[1] Amberg, G. and Homsy, G. (1993). Nonlinear analysis of buoyant convection in binary solidification with application to channel formation. *Journal of Fluid Mechanics*, 252 79-98.

[2] Anderson, D. and Worster, M. G. (1995). Weakly nonlinear analysis of convection in mushy layers during the solidification of binary alloys. *Journal of Fluid Mechanics*, 302 307-331.

[3] Chandrasekhar, S. (1981). Hydrodynamic and Hydromagnetic Stability. Dover New York.

[4] Bhatta D., Muddamallappa M. S., Riahi D.N., on perturbation and marginal stability analysis of magneto-convection in active mushy layer, accepted for publication in *Transport in Porous Media.*

[5] Bhatta D., Muddamallappa M. S., Riahi D.N., Effect of non-uniform magnetic field on convective instability of a mushy layer with variable permeability, in review *International Journal of Engineering Science.*

[6] Chen, F. and Chen, C. (1991). Experimental study of directional solidification of aqueous ammonium chloride solution. *Journal of Fluid Mechanics*, 227:567-586.

[7] Chen C.F.(1995) Experimental study of convection in a mushy layer during directional solidification, *Journal of Fluid Mechanics*, 293:81-98.

[8] Chung, C. and Chen, F. (2000). Onset of plume convection in mushy layers. *Journal of Fluid Mechanics*, 408:53-82.

[9] Cheney W., Kincaid D.(2008) Numerical Mathematics and Computing, Thomson Brooks/Co. 6th edition.

[10] Copley, S., Giamei, A., Johnson, S., and Hornbecker, M. (1970). The origin of freckles in unidirectionally solidified castings. *Metallurgical Transactions*, 1:2193-2204.

[11] Davis S. H. (2001). Theory of solidification. Cambridge University Press.

[12] Emms, P. and Fowler, A. (1994). Compositional convection in the solidification of binary alloys. *Journal of Fluid Mechanics*, 262:111-139.

[13] Fowler, A. (1985). The formation of freckles in binary alloys. *Journal of Applied Mathematics*, 35:159-174.

[14] Hills, R., Loper, D., and Roberts, P. (1983). A thermodynamically consistent model of a mushy zone. *Quarterly Journal of Mechanics and Applied Mathematics*, 36(4) 505-539.

[15] Huppert, H. and Worster, M. (1985). Dynamic solidification of a binary melt. *Nature* 314:703-707.

[16] Huppert, H. E. (1990). The fluid mechanics of solidification. *Journal of Fluid Mechanics* 212:209-240.

[17] Iooss, G. and Joseph, D. (1990). Elementary Stability and Bifurcation Theory. Springer 2nd edition.

[18] Muddamallappa M.S., Bhatta D., Riahi D.N. (2009) Numerical investigation on marginal stability and convection with and without magnetic field in a mushy layer, *Transport in Porous Media*, 79, 301-317

[19] Muddamallappa M. S., Bhatta D., Riahi D.N., Linear convective stability in a mushy layer with non-uniform magnetic field and permeable mush-liquid interface, accepted for publication in *Journal of Porous Media*.

[20] Okhuysen B.S. (2005) Analytical and computational studies of convection in solidifying binary Media, Ph.D. thesis, Department of Theoretical and Applied Mechanics, University of Illinois at Urbana-Champaign, USA.

[21] Okhuysen B.S., Riahi D.N.(2008a) On weakly nonlinear convection in mushy layers during solidification of alloys, *Journal Fluid Mechanics*. 596, 143-167.

[22] Okhuysen B.S., Riahi D.N.(2008b) Flow instabilities of liquid and mushy region during alloy solidification and under high gravity environment induced by rotation, *Int. J. Eng. Sci.* 46, 189-201.

[23] Riahi D.N.(2000) Effects of a vertical magnetic field on chimney convection in a

mushy layer *J. Crystal Growth*, 216, 501-511.

[24] Riahi D.N.(2001) Effects of centrifugal and Coriolis forces on a hydromagnetic chimney convection in a mushy layer, *J. Crystal Growth*, 226, 393-405.

[25] Riahi, D. (2003). Nonlinear steady convection in rotating mushy layers. *Journal of Fluid Mechanics*, 485:279-306.

[26] Tait, S., Jahrling, K., and Jaupart, C. (1992). The planform of compositional convection and chimney formation in a mushy layer. *Nature*, 359:406-408.

[27] Vives, C., Perry, C. (1987). Effects of magnetically damped convection during the controlled solidification of metals and alloys. *Int. J. Heat Mass Transfer* 30(3), 479–496.

[28] Worster, M. G. (1986). Solidification of an alloy from a cooled boundary. *Journal of Fluid Mechanics*, 167:481-501.

[29] Worster, M. G. (1991). Natural convection in a mushy layer. *Journal of Fluid Mechanics*, 224:335-359.

[30] Worster, M. G. (1992). Instabilities of the liquid and mushy regions during solidification of alloys. *Journal of Fluid Mechanics*, 237:649-669.

[31] Worster, M.G.(1997). Convection in mushy layers. *Ann. Rev. Fluid Mechanics.* 29, 91–122.

BIOGRAPHICAL SKETCH

Muddamallappa, Mallikarjunaiah S. was born in Siddapura, Karnataka, India. He obtained his Bachelors and Masters in Mathematics from Bangalore University, India in 2000 and 2003 respectively. He has teaching experience of four years and has taught undergraduate courses for students in Engineering College, Bangalore, India. He joined the Department of Mathematics, UTPA in Fall 2007 to pursue Masters in Mathematics.